First-trimester 3D power Doppler imaging markers of utero-placental vascular development are associated with placental weight and diameter at birth: the Rotterdam Periconception Cohort

Vos, E.S. de; Meeren, L.E. van der; Koning, A.H.J.; Nikkels, P.G.J.; Steegers, E.A.P.; Steegers-Theunissen, R.P.M.; Mulders, A.G.M.G.J.

Placenta 148 (2024) 44–52

Contents lists available at ScienceDirect

Placenta

journal homepage: www.elsevier.com/locate/placenta

First-trimester 3D power Doppler imaging markers of utero-placental vascular development are associated with placental weight and diameter at birth: The Rotterdam Periconception Cohort

Eline S. de Vos [a], Lotte E. van der Meeren [b,c], Anton H.J. Koning [b], Peter G.J. Nikkels [d], Eric A.P. Steegers [a], Régine P.M. Steegers-Theunissen [a], Annemarie G.M.G.J. Mulders [a,*]

[a] Department of Obstetrics and Gynecology, Erasmus MC University Medical Center, PO Box 2040, 3000 CA, Rotterdam, the Netherlands
[b] Department of Pathology, Erasmus MC University Medical Center, PO Box 2040, 3000 CA, Rotterdam, the Netherlands
[c] Department of Pathology, Leiden University Medical Center, PO Box 9600, 2300 RC, Leiden, the Netherlands
[d] Department of Pathology, University Medical Center Utrecht, H04.312, PO Box 85500, 3505 GA, Utrecht, the Netherlands

ARTICLE INFO

Keywords:
Human
Imaging
Histology
3D power Doppler ultrasound
Virtual reality
Placenta

ABSTRACT

Introduction: Early utero-placental vascular development impacts placental development and function throughout pregnancy. We investigated whether impaired first-trimester utero-placental vascular development is associated with pathologic features of the postpartum placenta.

Methods: In this prospective observational study of 65 ongoing pregnancies, we obtained three-dimensional power Doppler ultrasounds of the placenta at 7, 9 and 11 weeks of gestation. We applied VOCAL software to measure placental volume (PV), virtual reality based segmentation to measure utero-placental vascular volume (uPVV) and applied a skeletonization algorithm to generate the utero-placental vascular skeleton (uPVS). Vascular morphology was quantified by assigning a morphologic characteristic to each voxel in the uPVS (i.e. end-, bifurcation-, crossing- or vessel point). Following delivery, placentas were measured and histologically examined according to the Amsterdam criteria to assess maternal vascular malperfusion (MVM). We used linear mixed models to estimate trajectories of PV, uPVV and uPVS development. Multivariable linear regression analysis with adjustments for confounders was used to evaluate associations between PV, uPVV and uPVS development and features of the postpartum placenta.

Results: We observed no associations between first-trimester PV development and measurements of the postpartum placenta. Increased first-trimester utero-placental vascular development, reflected by uPVV ($\beta = 0.25$ [0.01; 0.48]), uPVS end points ($\beta = 0.25$ [0.01; 0.48]), bifurcation points ($\beta = 0.22$ [0.05; 0.37]), crossing points ($\beta = 0.29$ [0.07; 0.52]) and vessel points ($\beta = 0.09$ [0.02; 0.17]) was positively associated with the postpartum placental diameter. uPVV was positively associated with postpartum placental weight. No associations were found with MVM.

Discussion: Development of the first-trimester utero-placental vasculature is associated with postpartum placental size, whereas placental tissue development contributes to a lesser extent.

1. Introduction

For decades, histopathologic evaluation of the placenta, obtained following delivery or termination of pregnancy, has been our primary source of knowledge of the pathophysiology of placenta-related pregnancy complications [1,2]. Placentas from pregnancies with a placenta-related complication, including preeclampsia, fetal growth restriction and preterm birth, are characterized by macroscopic and microscopic histological aberrations. Macroscopically, placentas from complicated pregnancies present with lower weight and smaller disk dimensions [3–6]. Microscopically, these placentas often show signs within the spectrum of maternal vascular malperfusion, i.e. ischemia, infarction and accelerated maturation as a result of defective spiral artery remodeling [7,8]. As it is practically impossible to obtain placental biopsies during gestation, the clinical applicability of placental histology for antepartum screening of placenta-related complications is limited.

On the other hand, ultrasound techniques provide low-cost and

* Corresponding author. Erasmus MC University Medical Center, Department of Obstetrics and Gynecology, PO Box 2040, 3000 CA, Rotterdam, the Netherlands.
E-mail address: a.mulders@erasmusmc.nl (A.G.M.G.J. Mulders).

https://doi.org/10.1016/j.placenta.2024.01.019
Received 18 September 2023; Received in revised form 14 January 2024; Accepted 30 January 2024
Available online 8 February 2024

Abbreviations

3D	three-dimensional
BMI	body mass index
CRL	crown rump length
FR	fetal reactivity
GA	gestational age
ICSI	intracytoplasmic sperm injection
IVF	in vitro fertilization
LMP	last menstrual period
MVM	maternal vascular malperfusion
PD	power Doppler
PV	placenta volume
uPVV	utero-placental vascular volume
uPVS	utero-placental vascular skeleton
VOCAL	virtual organ computer-aided analysis
VR	virtual reality

noninvasive opportunities for early screening of pregnancy complications and are widely used in antenatal care. In the last decade, multiple studies have validated the first-trimester placental volume (PV) measurement using three-dimensional (3D) ultrasound and Virtual Organ Computer-aided AnaLysis (VOCAL$^{(TM)}$) [9–12]. A growing number of studies investigate the feasibility of using three-dimensional (3D) power Doppler (PD) ultrasound for assessment of utero-placental vascular development and function [13–18]. Recently, first-trimester 3D PD ultrasound was combined with virtual reality (VR) based segmentation and a skeletonization algorithm to measure utero-placental vascular volume (uPVV) and generate the utero-placental vascular skeleton (uPVS) as imaging markers of early (maternal) utero-placental vascular development [19,20]. Using these imaging markers, previous studies show that altered first-trimester utero-placental vascular development, including smaller absolute volumetric and morphologic development and increased density of vascular branching, is associated with the occurrence of placenta-related complications and disturbed embryonic and fetal growth [20–23].

Associations between imaging markers of first-trimester utero-placental vascular development and pregnancy outcomes suggest that early utero-placental vascular development, rather than placental stromal tissue development, impacts the development and function of the placenta throughout pregnancy. This hypothesis may be further substantiated by research comparing imaging markers of early placental (vascular) development with histopathologic features in the postpartum placenta. In the present study, we aim to investigate whether impaired first-trimester utero-placental vascular development, assessed with virtual imaging markers, is associated with pathologic features in the postpartum placenta in a prospective hospital-based cohort of pregnancies with and without placenta-related complications.

2. Methods

2.1. Study design

We used data from the VIRTUAL Placenta cohort, a subcohort embedded in the ongoing prospective Rotterdam Periconception Cohort (Predict study) [24,25]. Women were enrolled from a tertiary referral hospital between January 2017 and March 2018, if they were at least 18 years old, carried a singleton pregnancy of less than 10 weeks gestational age (GA), and gave written informed consent. Naturally conceived pregnancies as well as pregnancies achieved via in vitro fertilization (IVF) with or without intracytoplasmic sperm injection (ICSI) were eligible for inclusion. Women were excluded from analysis in case of oocyte donation and/or miscarriage. Upon inclusion, participants were required to complete a questionnaire detailing their general characteristics, medical and obstetrical history and lifestyle behaviors.

At least two study visits were arranged for each participant in the first trimester at 7, 9 and/or 11 weeks GA. At each visit transvaginal 3D PD ultrasound scans of the whole gestational sac including the placenta and utero-placental vasculature were acquired using the GE Voluson E8 (GE, Zipf, Austria). Standardized ultrasound settings were previously described (quality: max; pulse repetition frequency (PRF): 0.6; wall motion filter (WMF): low1; compound resolution imaging (CRI): off; power Doppler (PD) gain: −8.0) [19]. Ultrasound examinations were performed according to international guidelines on safe use of Doppler ultrasound in the first trimester of pregnancy (ALARA-principle) [26].

Body mass index (BMI) was determined during the first study visit using protocoled measurements of height and weight. Within 1 month after giving birth, participants completed a questionnaire about their pregnancy outcomes, which was validated with data from medical delivery records.

2.2. Pregnancy dating

For naturally conceived pregnancies in regular cycles with a duration between 25 and 35 days, GA was calculated from the first day of last menstrual period (LMP). In case of unknown LMP or irregular cycle, GA was calculated from Crown-Rump-Length (CRL). If the two methods varied >6 days, the CRL-based GA was assumed the true GA. For fresh IVF/ICSI conceived pregnancies, GA was calculated from oocyte pick-up day +14 days. In case of cryopreserved embryo transfer, GA was calculated from transfer date +19 days.

2.3. Imaging markers of the first-trimester utero-placental vascular development

Image quality was assessed on a four-point scale ranging between zero (optimal) and three (unusable) based on the presence of artefacts, the ability to discriminate between myometrium and trophoblastic tissue, and completeness of the placenta. Images with a quality score of three were excluded from the analyses.

The placental volume (PV) was measured using Virtual Organ Computer-aided AnaLysis (VOCAL) software according to the previously published study protocol [19]. In short, the placental outline, identified based on differences in echogenicity between trophoblast and myometrium, was repeatedly traced in rotational steps of 15° to calculate total pregnancy volume. Likewise, the gestational sac contours were traced to calculate the gestational sac volume. The gestational sac volume was subtracted from the total pregnancy volume to calculate the PV (cm^3) [27].

The utero-placental vascular volume (uPVV) was measured using a virtual reality (VR) desktop system with the V-Scope volume rendering application. First, the threshold for the 8-bit Doppler magnitude data was set at a value of 100, thereby only including voxels with a PD signal intensity between 100 and 255 in subsequent vascular volume measurements. Power Doppler artefacts were removed with a virtual eraser. Then, by visually identifying the embryonic structures and differences in tissue echogenicity between uterus and placenta, VR based segmentation was used to erase the PD signal in the embryo, the umbilical cord and the uterine tissue surrounding the placenta. After this, the V-Scope application automatically calculated the volume of all PD voxels within the VR based segmentation of the placenta to measure the uPVV (cm^3), as published previously [19].

The utero-placental vascular skeleton (uPVS) was generated by applying a skeletonization algorithm to the binary uPVV segmentations [20]. The skeletonization algorithm repeatedly peels off the outermost layer of voxels of the PD signal, reducing the diameter of the PD signal at each point in the vascular network until one central voxel remains, thereby creating a network-like structure representing the vascular morphology [20]. Following the construction of the network, the

skeletonization algorithm classifies each 26-connected voxel based on the number of neighboring voxels as either an endpoint (1 neighbor), a normal vessel point (2 neighbors), a bifurcation point (3 neighbors) or a crossing point (4 neighbors). Voxels with more than 4 neighbors are considered an artefact caused by 'hollow' spaces in the segmentation and are excluded from the analyses. Furthermore, the algorithm measures total network length and average vascular thickness (mm). These 6 uPVS characteristics represent absolute morphologic development of the first-trimester utero-placental vasculature.

Finally, we calculated ratios of the uPVS end-, bifurcation- and crossing points to the uPVV to identify 3 imaging markers to represent density of vascular branching in the utero-placental vascular volume. Women who had no PV, uPVV or uPVS measurement available, were excluded from analysis.

Given the small contribution of embryonic vascular structures to the VR based segmentation and the restricted presence of embryonic flow in the first trimester, we assume the attribution of the embryonic blood space to the uPVV and the uPVS is limited. Therefore, we consider the uPVV and uPVS mainly include the vasculature of the maternal spiral and basal arteries and of the arteriovenous shunts within the most distal section of the utero-placental circulation [19,20].

2.4. Histologic assessment of the postpartum placenta

All postpartum placentas were macroscopically and microscopically examined according to the internationally acknowledged Amsterdam criteria by two perinatal pathologists (LvdM, PN) [28]. Gross examination included measurements of placental weight (g) and placental disk dimensions, more specifically maximum diameter and thickness (cm) [28]. For microscopic inspection, we sampled multiple locations from each placenta, including the extra-placental membranes, umbilical cord and full-thickness sections of the placental parenchyma [28]. Microscopic findings thought indicative of *maternal vascular malperfusion* (MVM) (yes/no) include ischemia, infarction and acute atherosis. Accelerated maturation was not scored because of the large proportion of term placentas in our population. Microscopic signs of fetal thrombosis (fetal vascular malperfusion) and fetal hypoxia were considered indicative of *fetal reactivity* (FR) (yes/no). Inflammation was scored (yes/no) when signs of chorioamnionitis, intervillositis, chronic deciduitis, funiculitis, chronic villitis of unknown etiology or sustained villitis were present. Finally, maturation was classified as delayed maturation or normal maturation.

2.5. Statistical analysis

Baseline characteristics were presented as mean with standard deviation. If needed, non-volumetric parameters were transformed using a square root transformation to approximate a normal distribution. For volumetric parameters and ratios, a cubic root and natural log transformation were used respectively. For each variable we selected the transformation of which the histogram most closely approximated a normal distribution.

Multivariable linear mixed models were used to summarize the PV, uPVV and uPVS measurements at 7, 9, and 11 weeks gestational age for each participant into individual PV, uPVV and uPVS development trajectories using a quadratic relation with GA. In these models, we allowed for subject-specific intercepts and slopes as random effects. The random effects were used as summaries representing first-trimester utero-placental vascular morphologic development.

Hereafter, the summaries of first-trimester utero-placental vascular morphologic development (PV, uPVV and uPVS characteristics) were used as covariates in the multivariable linear regression analysis for continuous outcome measures (placental weight, maximum placental diameter and placental thickness) and in logistic regression analysis for binominal outcome measures (MVM, FR, inflammation and delayed maturation).

We performed multivariable linear mixed models to estimate the association between imaging markers of utero-placental vascular development, assessed by PV, uPVV and uPVS, and histopathologic features of the postpartum placenta. We constructed model 1 (adjusted for GA at birth); model 2 (model 1 additionally adjusted for maternal age, BMI, parity, conception mode, fetal sex and periconceptional alcohol consumption, smoking and folic acid supplement use). For placental disk dimensions we also constructed model 3 (model 2 additionally adjusted for placental weight). Possible confounders were selected based on literature, characteristics of the study population and discussion amongst authors.

All analyses were performed using SPSS (version 25.0; SPSS Inc., Chicago, IL, USA) and R (version 4.0.2, R Core Team, Vienna, Austria, 2020), p-values <0.05 were considered statistically significant.

3. Results

3.1. Study population

A total of 241 women were enrolled in the VIRTUAL Placenta study. A flow chart of the study population is depicted in Supplementary Fig. S1. One woman withdrew from the study. We excluded 175 women from the analyses because of miscarriage (n = 22), oocyte donation (n = 4) or because the placenta was not available for histopathologic examination (n = 149). Finally, 65 women were included in this study. Table 1 shows the baseline characteristics of the study population. Participants were on average 32.4 years of age, 41% was nulliparous and 20% of the pregnancies was achieved via IVF-ICSI. The average GA at birth was 261 days (37^{+2} weeks). Table 2 summarizes the histopathological features in the postpartum placentas. From the 24 women clinically diagnosed with any

Table 1
Baseline characteristics of study population (n = 65).

	Total cohort (n = 65) Mean (SD) or n (%)
Maternal characteristics	
Age (years)	32.4 (4.2)
Nulliparous (yes)	27 (41.5%)
IVF/ICSI (yes)	13 (20.0%)
Geographic origin	
Dutch	48 (73.8%)
Western	2 (3.1%)
Non-Western	13 (20.0%)
Educational Level	
Low	4 (6.2%)
Intermediate	22 (33.8%)
High	37 (56.9%)
BMI at first visit, (kg/m^2)	26.4 (6.1)
Folic acid supplement use (yes)	50 (76.9%)
Alcohol consumption (yes)	15 (23.1%)
Smoking (yes)	13 (20.0%)
Neonatal outcomes	
Fetal sex (boys)	33 (50.8%)
GA at birth (days)	261 (29)
Birth weight (grams)	2995 (733)
Hoftiezer percentiles	43 (32)
Congenital anomalies	2 (3.1%)
Placenta-related complications[a]	24 (36.9%)
PIH[b]	4 (6.2%)
PE[b]	4 (6.2%)
FGR[b]	8 (12.3%)
SGA[b]	10 (15.4%)
PTB[b]	11 (16.9%)

IVF = in vitro fertilization. ICSI = intracytoplasmic sperm injection. BMI = body-mass index. GA = gestational age. PIH = pregnancy induced hypertension. PE = preeclampsia. FGR = fetal growth restriction. SGA = small-for-gestational-age. PTB = preterm birth.

[a] Placenta-related complications are specified as PIH or PE and/or FGR, PTB and SGA.

[b] Diagnoses may be overlapping.

Table 2
Histopathological features of the delivered placenta.

	Total cohort (n = 65) Mean (SD) or n (%)
Macroscopic characteristics	
Placental weight (g)	436 (118)
Placenta weight percentiles	
<10th	20 (30.8%)
10th–25th	20 (30.8%)
26th–50th	6 (9.2%)
51st–75th	2 (3.1%)
76th - 90th	7 (10.8%)
>90th	10 (15.4%)
Maximum placental diameter (cm)	18.1 (3.2)
Placental thickness (cm)	2.2 (0.8)
Umbilical vessels, 3	64 (98.5%)
Coiling index	0.21 (0.10)
Cord diameter (cm)	1.39 (0.55)
Cord insertion	
Central	2 (3.1%)
Paracentral	60 (91.3%)
Marginal	2 (3.1%)
Velamentous	1 (1.5%)
Microscopic characteristics	
MVM	28 (43.1%)
Ischemia, yes[a]	25 (38.5%)
Infarction, yes[a]	13 (20.0%)
Atherosis, yes[a]	2 (3.1%)
FR	14 (21.5%)
Fetal hypoxia, yes[a]	12 (18.5%)
Fetal thrombosis, yes[a]	3 (4.6%)
Inflammation, yes	23 (35.4%)
Maturation, delayed	22 (33.8%)

MVM = maternal vascular malformation. FR = fetal reactivity.
[a] Microscopic features may be overlapping.

placenta-related complication, 14 (58.3%), 5 (20.8%), 12 (50.0%), and 7 (29.2%) placenta's showed signs of MVM, FR, inflammation and delayed maturation, respectively. In women without any placenta-related complication, the frequencies of MVM, FR, inflammation and delayed maturation were 14 (34.1%), 9 (22.0%), 11 (26.8%) and 15 (36.6%), respectively.

3.2. Macroscopic features

Associations between virtual imaging markers of first-trimester utero-placental vascular development and macroscopic features of the postpartum placenta are depicted in Table 3, Fig. 1 and Supplementary Table S2. First, we investigated the associations with placental weight. Both model 1 and 2 showed increased first-trimester uPVV development, but not PV development, was associated with higher placental weight of the postpartum placenta, see Table 3. Absolute maternal vascular morphologic development, estimated by trajectories of the uPVS characteristics, was positively associated with placental weight in model 2, not all associations were statistically significant. In model 1, first-trimester density of vascular branching was inversely associated with placental weight of the postpartum placenta. Similar associations were observed in the model 2, but were not statistically significant.

Next, we investigated associations with placental disk dimensions. Both model 1 and 2 showed increased uPVV development and increased absolute maternal vascular morphologic development, but not PV development, were associated with a larger maximum placental diameter of the postpartum placenta, see Fig. 1 and Supplementary Table S2. In model 3, we observed similar associations, but not all associations were statistically significant. We repeated these analyses for placental thickness, but found no associations, see Supplementary Table S2.

3.3. Microscopic features

The associations between first-trimester imaging markers of utero-placental vascular development and microscopic features of the postpartum placenta are depicted in Table 4. We found no associations between imaging markers of first-trimester utero-placental vascular development and MVM, FR, inflammation or delayed maturation in both model 1 and model 2, see Table 4 (data of model 1 not shown).

4. Discussion

This study demonstrates that increased first-trimester of utero-placental vascular development, assessed by virtual imaging markers, is associated with increased weight and diameter of the postpartum placenta. We observed no associations with histological features of maternal vascular malperfusion or fetal reactivity.

4.1. Macroscopic features

The positive associations between imaging markers of first-trimester utero-placental vascular development and measurements of the

Table 3
The association between virtual imaging markers of first-trimester utero-placental vascular development and weight of the delivered placenta (n = 65).

	Model 1			Model 2		
	Effect size	95% CI	p-value	Effect size	95% CI	p-value
	Placental weight (g)			Placental weight (g)		
Imaging markers representing absolute placental volume development and absolute utero-placental vascular volume development						
RI $\sqrt[3]{}$ PV (cm^3) (n = 58)	21.79	−53.73; 97.32	0.565	22.39	−56.72; 101.51	0.572
RS $\sqrt[3]{}$ PV (cm^3) (n = 58)	5391.73	−918.98; 11702.45	0.092	5048.12	−1383.45; 11479.68	0.121
RI $\sqrt[3]{}$ uPVV (cm^3) (n = 63)	**128.10**	**37.98; 218.22**	**0.006***	151.30	**52.31; 250.28**	**0.003***
Imaging markers representing absolute morphologic development of the utero-placental vasculature						
RI $\sqrt{}$ uPVS end points (n) (n = 63)	2.00	−5.55; 9.56	0.598	4.04	−4.09; 12.18	0.324
RI $\sqrt{}$ uPVS bifurcation points (n) (n = 63)	4.14	−1.15; 9.43	0.122	5.77	−0.06; 11.60	0.052
RI $\sqrt{}$ uPVS crossing points (n) (n = 63)	5.05	−1.83; 11.92	0.147	7.65	−0.16; 15.46	0.055
RI $\sqrt{}$ uPVS vessel points (n) (n = 63)	1.79	−0.55; 4.13	0.132	2.47	−0.10; 5.04	0.059
RI $\sqrt{}$ uPVS total length (mm) (n = 63)	2.31	−0.32; 4.93	0.084	**3.23**	**0.28; 6.17**	**0.032***
RI $\sqrt{}$ uPVS average thickness (mm) (n = 63)	−40.49	−454.25; 373.26	0.845	−110.42	−545.01; 324.18	0.612
Imaging markers representing density of vascular branching						
RI *log* density of end points (n/cm^3) (n = 63)	**−95.70**	**−164.92; -26.48**	**0.008***	**−93.71**	**−169.05; -18.37**	**0.016***
RI *log* density of bifurcation points (n/cm^3) (n = 63)	**−141.79**	**−255.10; -28.47**	**0.015***	−118.83	−240.82; 3.16	0.056
RI *log* density of crossing points (n/cm^3) (n = 63)	**−150.21**	**−292.73; -7.69**	**0.039***	−107.32	−260.39; 45.75	0.165

Model 1: adjusted for gestational age at birth. Model 2: Model 1 additionally adjusted for maternal age, BMI, parity, conception mode, fetal sex and periconceptional alcohol consumption, smoking and folic acid supplement use. RI = random intercept. RS = random slope. PV = placental volume. uPVV = utero-placental vascular volume. uPVS = utero-placental vascular skeleton. *significance at p-value<0.05.

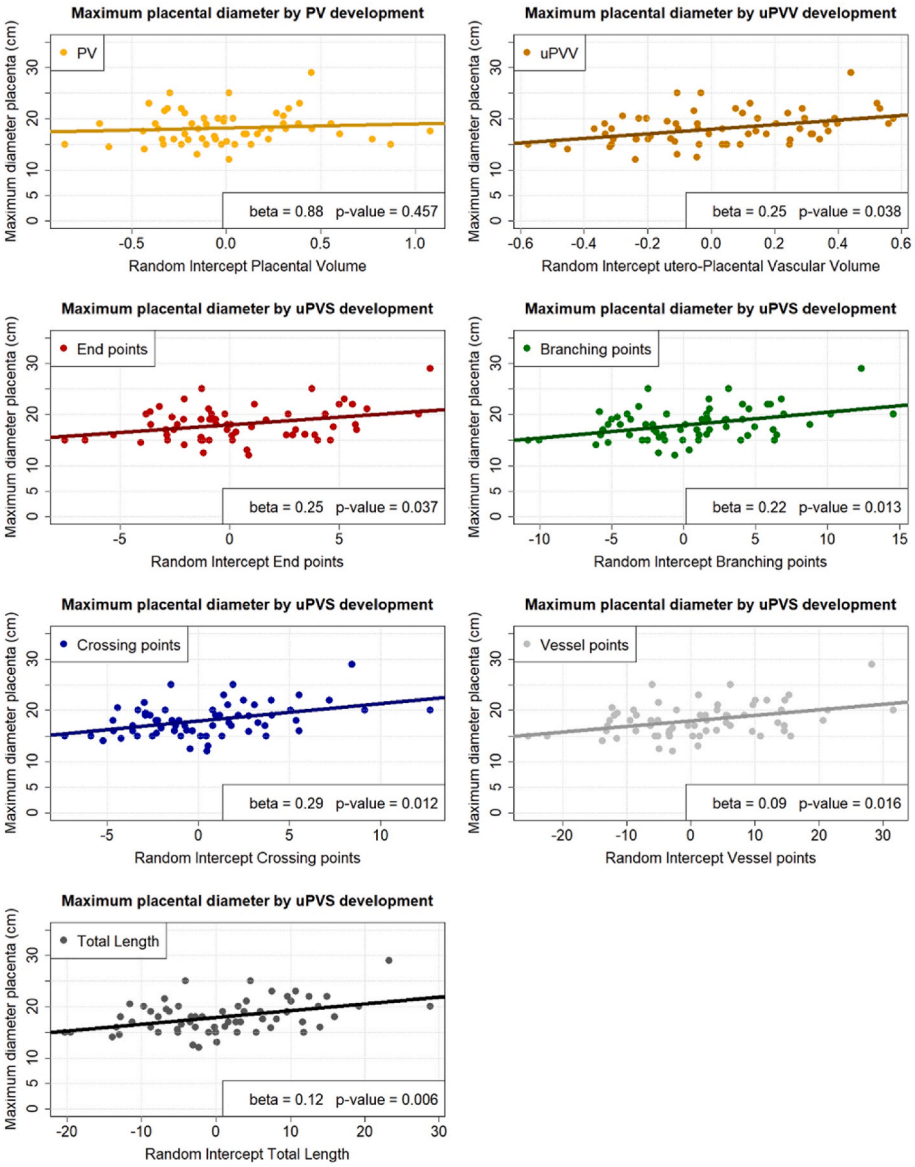

Fig. 1. The association between first-trimester placental volume (PV) development, first-trimester utero-placental vascular volume (uPVV) development and first-trimester utero-placental vascular skeleton (uPVS) development and the maximum placental diameter at delivery. Presented are the beta's and p-values of model 2: adjusted for gestational age at birth, maternal age, BMI, parity, conception mode, fetal sex and periconceptional alcohol consumption, smoking and folic acid supplement use. Significance at p-value<0.05.

postpartum placenta suggests that early maternal utero-placental vascular development impacts placental size across pregnancy. These findings support the general assumption that a small placental size and maternal vascular malperfusion lesions of the placenta in late pregnancy arise from aberrations in the utero-placental vascular development from the first trimester of pregnancy onwards [1,8,29,30]. The placental villous tissue, invading trophoblast and decidua form the main part of PV. The fact that in our study first trimester PV development is not associated with measurements of the postpartum placenta at birth supports our hypothesis that development of the placenta during the second and third trimester is mainly affected by the utero-placental (maternal) vasculature and to a lesser extent by the placental tissue in the first trimester.

We cannot differentiate whether the increased vascular development (as measured with the uPVV and uPVS) results from newly formed vessels or whether increased blood flow reaches the detection threshold in a larger proportion of the existing vasculature or a combination of both factors. Regardless, using the uPVV and uPVS we observed that increased detection of the utero-placental vasculature in the first-trimester is associated with increased placental size at delivery. These results imply that first-trimester utero-placental vascular development is important for placental development during later pregnancy.

We found only the study of Odibo et al. that investigated associations between first trimester ultrasound markers of PV and maternal vascularity indices and morphologic features of the postpartum placenta. Similar to our results, they observed no associations between first trimester PV and the volume or villous surface area of the postpartum placenta, but they did find negative associations between uterine artery pulsatility index as indirect measure of utero-placental vascular development and placental volume at birth [31]. These findings further substantiate our hypothesis that functional development of the utero-placental vasculature is more important for development of the placenta during later gestation than the amount of placental villi during the first trimester of pregnancy.

A larger placental diameter of the postpartum placenta is indicative of an increased placental disk surface, which implies a larger portion of

Table 4
The association between virtual imaging markers of first-trimester utero-placental vascular development and microscopic features of the delivered placenta (n = 65).

	Model 2			Model 2		
	Effect size	95% CI	p-value	Effect size	95% CI	p-value
	MVM			Inflammation		
Imaging markers representing absolute placental volume development and absolute utero-placental vascular volume development						
RI $\sqrt[3]{}$ PV (cm3) (n = 58)	−0.26	−1.85; 1.27	0.739	−0.03	−1.70; 1.64	0.967
RS $\sqrt[3]{}$ PV (cm3) (n = 58)	−4.15	−133.81; 124.18	0.948	−9.61	−155.87; 129.35	0.891
RI $\sqrt[3]{}$ uPVV (cm3) (n = 63)	−0.29	−2.47; 1.85	0.787	0.04	−2.37; 2.45	0.968
Imaging markers representing absolute morphologic development of the utero-placental vasculature						
RI $\sqrt{}$ uPVS end points (n) (n = 63)	0.05	−0.11; 0.22	0.544	0.06	−0.14; 0.25	0.565
RI $\sqrt{}$ uPVS bifurcation points (n) (n = 63)	0.01	−0.11; 0.14	0.812	0.03	−0.11; 0.16	0.672
RI $\sqrt{}$ uPVS crossing points (n) (n = 63)	−0.02	−0.18; 0.15	0.848	0.09	−0.09; 0.28	0.324
RI $\sqrt{}$ uPVS vessel points (n) (n = 63)	0.01	−0.04; 0.07	0.693	0.01	−0.05; 0.07	0.779
RI $\sqrt{}$ uPVS total length (mm) (n = 63)	−0.00	−0.07; 0.06	0.914	0.02	−0.05; 0.09	0.514
RI $\sqrt{}$ uPVS average thickness (mm) (n = 63)	−5.80	−17.02; 3.25	0.245	2.42	−7.01; 12.97	0.616
Imaging markers representing density of vascular branching						
RI *log* density of end points (n/cm3) (n = 63)	0.41	−1.18; 2.05	0.616	0.44	−1.44; 2.40	0.650
RI *log* density of bifurcation points (n/cm3) (n = 63)	1.34	−1.21; 4.04	0.309	1.03	−1.92; 4.15	0.498
RI *log* density of crossing points (n/cm3) (n = 63)	1.29	−1.80; 4.53	0.416	2.84	−0.71; 6.73	0.138
	FR			Maturation, delayed		
Imaging markers representing absolute placental volume development and absolute utero-placental vascular volume development						
RI $\sqrt[3]{}$ PV (cm3) (n = 58)	−0.09	−2.46; 2.14	0.939	−0.22	−2.15; 1.64	0.816
RS $\sqrt[3]{}$ PV (cm3) (n = 58)	−78.01	−282.85; 109.69	0.418	159.69	−13.90; 368.38	0.092
RI $\sqrt[3]{}$ uPVV (cm3) (n = 63)	1.97	−1.08; 5.43	0.224	1.91	−0.70; 4.80	0.167
Imaging markers representing absolute morphologic development of the utero-placental vasculature						
RI $\sqrt{}$ uPVS end points (n) (n = 63)	0.14	−0.09; 0.41	0.232	−0.02	−0.22; 0.17	0.849
RI $\sqrt{}$ uPVS bifurcation points (n) (n = 63)	0.01	−0.11; 0.14	0.812	0.06	−0.08; 0.21	0.418
RI $\sqrt{}$ uPVS crossing points (n) (n = 63)	0.25	−0.01; 0.55	0.059	0.09	−0.10; 0.30	0.337
RI $\sqrt{}$ uPVS vessel points (n) (n = 63)	0.08	−0.00; 0.19	0.076	0.02	−0.04; 0.09	0.528
RI $\sqrt{}$ uPVS total length (mm) (n = 63)	0.08	−0.01; 0.20	0.112	0.03	−0.04; 0.11	0.421
RI $\sqrt{}$ uPVS average thickness (mm) (n = 63)	−6.87	−24.91; 5.96	0.386	−4.23	−16.43; 5.81	0.429
Imaging markers representing density of vascular branching						
RI *log* density of end points (n/cm3) (n = 63)	−0.66	−5.04; 1.63	0.568	−1.49	−3.63; 0.45	0.146
RI *log* density of bifurcation points (n/cm3) (n = 63)	1.34	−1.21; 4.04	0.309	−1.91	−5.20; 1.17	0.232
RI *log* density of crossing points (n/cm3) (n = 63)	1.93	−2.64; 7.06	0.424	−1.55	−5.75; 2.38	0.443

Model 2: adjusted for gestational age at birth, maternal age, BMI, parity, conception mode, fetal sex and periconceptional alcohol consumption, smoking and folic acid supplement use. MVM = maternal vascular malformation. FR = fetal reactivity. RI = random intercept. RS = random slope. PV = placental volume. uPVV = utero-placental vascular volume. uPVS = utero-placental vascular skeleton. *significance at p-value<0.05.

the uterine surface is covered by the placenta. Consequently, the potential number of remodeled spiral arteries supplying the placenta increases, and the placental capacity for maternal-fetal exchange improves [32]. Several studies show that a small placental disk surface and small placental thickness are associated with decreased placental function, reflected by a higher placental weight to birth weight ratio, and are subsequently associated with lower Apgar scores [32–35]. Other studies found a reduced placental weight and surface area, but not thickness, to be associated with a lower birth weight [36–38]. Similarly, we found associations with placental weight and diameter, but we did not find any associations with placental thickness. Placental thickness, however, differs according to in-vivo (during pregnancy) and ex-vivo (after delivery) circumstances. Fig. 2 illustrates how in-vivo placental thickness measured via ultrasound (33 mm) is different with the ex-vivo thickness of the postpartum placenta (25 mm). This difference might be explained by detachment of the uterine wall and subsequent loss of 'pressurized' maternal flow in the intervillous space and the following formalin fixation of the placenta [39–41]. Consequently, placental thickness could be considered a less accurate marker of placental functioning, explaining the lack of and an association with our imaging markers of utero-placental vascular development.

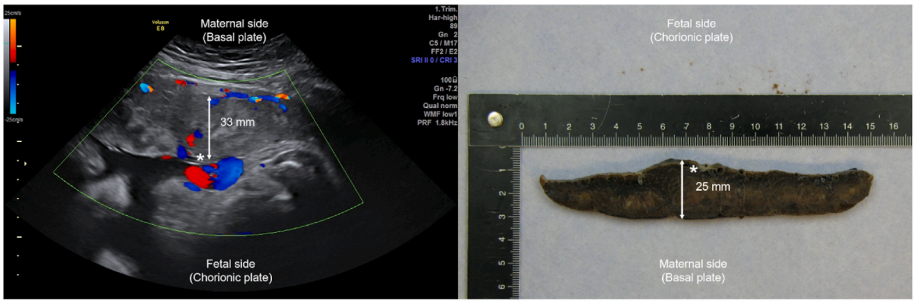

Figure 2. Placental thickness measured via ultrasonography vs in the delivered placenta. Left: Placental thickness of 33 mm measured via ultrasonography at 37 + 3 weeks gestational age (1 day before delivery per cesarean section). Right: Placental thickness of 25 mm measured in the delivered placenta at 37 + 4 weeks gestational age (day of the delivery per cesarean section). * Marks umbilical cord insertion.

4.2. Microscopic features

We found no associations between imaging markers of first-trimester utero-placental vascular development and microscopic features of the postpartum placenta. To our knowledge, these associations have not previously been investigated. However, a few studies have investigated associations between first trimester maternal serum biomarkers of placental (vascular) development and placental pathology. These studies, conducted in larger cohorts of approximately 200 pregnancies, found decreased levels of pregnancy-associated plasma protein A (PAPP-A) and placental growth factor (PlGF) and increased levels of soluble fms-like tyrosine kinase-1 (sFLT-1) to be associated with an increased odds ratio of maternal vascular malperfusion (MVM), specifically in pregnancies with PE and SGA [42,43].

Despite the small size of our cohort, we observed a comparable incidence of MVM in our study population as reported by these two studies [42,43]. Moreover, we found a comparable incidence of MVM as a previously conducted large cohort study (n = 3074) with an incidence of MVM in the total cohort of 39.9% (vs 43.1% in our cohort), 52.3% MVM (vs 58.3% in our cohort) in their subgroup of pregnancies with hypertensive disorders and 36.4% (vs 34.1% in our cohort) in pregnancies without hypertensive disorders [44]. We therefore argue our cohort is representative, but underpowered to detect small effect sizes of the associations between imaging markers of first-trimester utero-placental vascular development and MVM. In addition, our sample size was too small to analyze the subgroup of pregnancies with placenta-related complications separately.

4.3. Strengths and limitations

This is the first study to investigate associations between the physiologic development of the first-trimester utero-placental vasculature using virtual imaging markers and histopathologic features of the postpartum placenta. The main strength of this study is the longitudinal collection of high quality sequential 3D PD ultrasounds in the early first trimester. The 3D ultrasounds were used to perform validated uPVV measurements (ICC above 0.80 and relative differences of less than 20%) [19] and to generate the uPVS, which we used as imaging markers of utero-placental vascular development [20].

Further, the histopathologic examination of all postpartum placentas was performed by two experienced perinatal pathologists (LvdM, PN). All examinations were performed according to the internationally acknowledged Amsterdam Criteria for placental lesions [28].

Despite the relatively large number of participants initially included in this study (n = 241), we only had a limited number of placentas available for histopathological examination (n = 65). This discrepancy largely results from the organization of obstetric healthcare in the Netherlands. Even though all participants received care in our tertiary referral hospital at the start of their pregnancy, patients are allowed and even encouraged to deliver in other health facilities according to their actual health risks. As a result, only a part of the study population delivered in our hospital and only those placentas were available for histopathologic examination.

Our small study population and number of covariates in our adjusted model might introduce some over adjustment. Model 1 (adjusted for GA at birth) shows no associations between first-trimester imaging markers and placental weight. However, model 2 (additionally adjusted for maternal age, BMI, parity, conception mode, fetal sex, periconceptional alcohol consumption, smoking, and folic acid supplement use) reveals borderline statistically significant positive associations. For other outcome measures of the postpartum placenta, models 1 and 2 yield similar results, suggesting that the positive associations between first-trimester imaging markers and placental diameter are unlikely to result from over adjustment.

The number of imaging markers tested in this study may give rise to concerns regarding the issue of multiple testing. However, prior research has consistently demonstrated strong correlations between the uPVV and uPVS an inverse association with density of vascular branching. Consequently, we contend that the consistent presence or absence of these associations can be considered as internal validation of our findings.

We have chosen to recruit our participants from a tertiary referral hospital to select a population with increased risk of developing a placenta-related complication. As a result, our study population contains a relatively high number of IVF-ICSI pregnancies, which might affect the generalizability of our results [25]. However, we believe it is unlikely that the direction of the associations will be different in the general population.

4.4. Future perspectives

In previous studies, increased uPVV development, increased absolute vascular development and decreased density of vascular branching in the first trimester were positively associated with embryonic and fetal growth and birth weight percentiles [21–23]. The interplay between first-trimester utero-placental vascular development, size of the postpartum placenta and early and late fetal growth, suggests potential for clinical applicability of early placental imaging markers to study early placental function. Our new ultrasound-derived imaging markers of utero-placental vascular development (the uPVV and uPVS) provide non-invasive opportunities to monitor aberrations in the utero-placental vascular development in early pregnancy in vivo [9,19,20]. Therefore, future research should investigate the clinical applicability of the uPVV and uPVS as markers for early detection of placenta-related complications.

In addition, application of the uPVV and uPVS to investigate the effect of prophylactic aspirin use on first-trimester utero-placental vascular development in vivo, might provide a valuable contribution to our understanding of aspirin prophylaxis and consequently benefit the debate on indications for administration, optimal dosage and gestational age at the start of treatment for the prevention of hypertensive disorders of pregnancy.

5. Conclusion

Using new imaging markers of utero-placental vascular development, the uPVV and uPVS, this study shows first-trimester of utero-placental vascular development, but not placental stromal tissue development, is associated with placental weight and diameter at delivery. The results of this study substantiate the importance of early utero-placental vascular development for adequate development and function of the placenta throughout pregnancy. As the uPVV and uPVS can be used to monitor first-trimester development of the utero-placental vasculature, they may be valuable as early indicators of placental function. The clinical applicability of these new imaging markers of utero-placental vascular development for early detection of placenta-related complications requires further investigation.

CRediT authorship contribution statement

Eline S. de Vos: Conceptualization, Data curation, Formal analysis, Methodology, Visualization, Writing – original draft. **Lotte E. van der Meeren:** Conceptualization, Data curation, Investigation, Methodology, Supervision, Writing – review & editing. **Anton H.J. Koning:** Conceptualization, Methodology, Software, Supervision, Writing – review & editing. **Peter G.J. Nikkels:** Conceptualization, Writing – review & editing. **Eric A.P. Steegers:** Conceptualization, Writing – review & editing. **Régine P.M. Steegers-Theunissen:** Conceptualization, Project administration, Resources, Writing – review & editing. **Annemarie G. M.G.J. Mulders:** Methodology, Supervision, Writing – review & editing.

Declaration of competing interest

The authors declare that they have no known competing financial interests or personal relationships that could have appeared to influence the work reported in this paper.

Acknowledgements

We thank all participants of the VIRTUAL Placenta study and Rotterdam Periconception Cohort and The Rotterdam Periconception Cohort team.

Appendix A. Supplementary data

Supplementary data to this article can be found online at https://doi.org/10.1016/j.placenta.2024.01.019.

References

[1] I. Brosens, P. Puttemans, G. Benagiano, Placental bed research: I. The placental bed: from spiral arteries remodeling to the great obstetrical syndromes, Am. J. Obstet. Gynecol. 221 (5) (2019) 437–456.
[2] I. Brosens, R. Pijnenborg, L. Vercruysse, R. Romero, The "Great Obstetrical Syndromes" are associated with disorders of deep placentation, Am. J. Obstet. Gynecol. 204 (3) (2011) 193–201.
[3] B. Vijayalakshmi, S. Kittali, Morphological changes of placenta in cases of pre-eclampsia and perinatal outcome, Int. J. Sci. Stud. 3 (5) (2015).
[4] B. Dahlstrom, P. Romundstad, P. Oian, L.J. Vatten, A. Eskild, Placenta weight in pre-eclampsia, Acta Obstet. Gynecol. Scand. 87 (6) (2008) 608–611.
[5] V. Visan, R.A. Balan, C.F. Costea, A. Carauleanu, R.M. Haba, M.S.C. Haba, D. G. Socolov, R.A. Mogos, C.M. Bogdanici, D. Nemescu, D.M. Tanase, M.D. Turliuc, A.I. Cucu, D.V. Scripcariu, B.F. Toma, R.M. Popovici, M. Ciocoiu, F.D. Petrariu, Morphological and histopathological changes in placentas of pregnancies with intrauterine growth restriction, Rom. J. Morphol. Embryol. 61 (2) (2020) 477–483.
[6] K.M. Chisholm, A.K. Folkins, Placental and clinical characteristics of term small-for-gestational-age neonates: a case-control study, Pediatr. Dev. Pathol. 19 (1) (2016) 37–46.
[7] J. Espinoza, R. Romero, Y. Mee Kim, J.P. Kusanovic, S. Hassan, O. Erez, F. Gotsch, N.G. Than, Z. Papp, C. Jai Kim, Normal and abnormal transformation of the spiral arteries during pregnancy, J. Perinat. Med. 34 (6) (2006) 447–458.
[8] G.J. Burton, E. Jauniaux, Pathophysiology of placental-derived fetal growth restriction, Am. J. Obstet. Gynecol. 218 (2S) (2018) S745–S761.
[9] A.D. Reus, H. El-Harbachi, M. Rousian, S.P. Willemsen, R.P. Steegers-Theunissen, E.A. Steegers, N. Exalto, Early first-trimester trophoblast volume in pregnancies that result in live birth or miscarriage, Ultrasound Obstet. Gynecol. 42 (5) (2013) 577–584.
[10] D. Meengeonthong, S. Luewan, S. Sirichotiyakul, T. Tongsong, Reference ranges of placental volume measured by virtual organ computer-aided analysis between 10 and 14 weeks of gestation, J. Clin. Ultrasound 45 (4) (2017) 185–191.
[11] B. Artunc Ulkumen, H.G. Pala, Y. Uyar, F.M. Koyuncu, Y. Bulbul Baytur, The assessment of placental volume and mean gray value in preeclamptic placentas by using three-dimensional ultrasonography, J. Matern. Fetal Neonatal Med. 28 (9) (2015) 1010–1013.
[12] W. Plasencia, E. Gonzalez-Davila, A. Gonzalez Lorenzo, M. Armas-Gonzalez, E. Padron, N.L. Gonzalez-Gonzalez, First trimester placental volume and vascular indices in pregnancies complicated by preeclampsia, Prenat. Diagn. 35 (12) (2015) 1247–1254.
[13] E. Jauniaux, S. Collins, G.J. Burton, Placenta accreta spectrum: pathophysiology and evidence-based anatomy for prenatal ultrasound imaging, Am. J. Obstet. Gynecol. 218 (1) (2018) 75–87.
[14] S. Mathewlynn, S.L. Collins, Volume and vascularity: using ultrasound to unlock the secrets of the first trimester placenta, Placenta 84 (2019) 32–36.
[15] V.H.J. Roberts, T.K. Morgan, P. Bednarek, M. Morita, G.J. Burton, J.O. Lo, A. E. Frias, Early first trimester uteroplacental flow and the progressive disintegration of spiral artery plugs: new insights from contrast-enhanced ultrasound and tissue histopathology, Hum. Reprod. 32 (12) (2017) 2382–2393.
[16] G.N. Stevenson, J.A. Noble, A.W. Welsh, L. Impey, S.L. Collins, Automated visualization and quantification of spiral artery blood flow entering the first-trimester placenta, using 3-D power Doppler ultrasound, Ultrasound Med. Biol. 44 (3) (2018) 522–531.
[17] W. Sun, J. Liu, Y. Zhang, A. Cai, Z. Yang, Y. Zhao, Y. Wang, Z. Cao, Q. Wei, Quantitative assessment of placental perfusion by three-dimensional power Doppler ultrasound for twins with selective intrauterine growth restriction in one twin, Eur. J. Obstet. Gynecol. Reprod. Biol. 226 (2018) 15–20.
[18] A.O. Odibo, K.R. Goetzinger, K.M. Huster, J.K. Christiansen, L. Odibo, M.G. Tuuli, Placental volume and vascular flow assessed by 3D power Doppler and adverse pregnancy outcomes, Placenta 32 (3) (2011) 230–234.
[19] I.F. Reijnders, A. Mulders, M.P.H. Koster, A.H.J. Koning, A. Frudiger, S. P. Willemsen, E. Jauniaux, G.J. Burton, R.P.M. Steegers-Theunissen, E.A. P. Steegers, New imaging markers for preconceptional and first-trimester utero-placental vascularization, Placenta 61 (2018) 96–102.
[20] E.S. de Vos, A.H.J. Koning, R.P.M. Steegers-Theunissen, S.P. Willemsen, B.B. van Rijn, E.A.P. Steegers, A. Mulders, Assessment of first-trimester utero-placental vascular morphology by 3D power Doppler ultrasound image analysis using a skeletonization algorithm: the Rotterdam Periconception Cohort, Hum. Reprod. (2022).
[21] I.F. Reijnders, A. Mulders, M.P.H. Koster, A.T.M. Kropman, E.S. de Vos, A.H. J. Koning, S.P. Willemsen, M. Rousian, E.A.P. Steegers, R.P.M. Steegers-Theunissen, First-trimester utero-placental (vascular) development and embryonic and fetal growth: the Rotterdam periconception cohort, Placenta 108 (2021) 81–90.
[22] M.A.G. deVosE, A.H.J. Koning, S.P. Willemsen, B.B. van Rijn, E.A.P. Steegers, R.P. M. Steegers-Theunissen, The utero-placental vascular skeleton and the association with Firsttrimester embryo development: the Rotterdam Periconception cohort, in: 69th Annual Meeting of the Society for Reproductive Investigation (SRI), Denver, CO, USA, 2022, p. 57A.
[23] M.A.G.E.S. Vos de, A.H.J. Koning, S.P. Willemsen, B.B. van Rijn, E.A.P. Steegers, R. P.M. Steegers-Theunissen, Features of First Trimester Uteroplacental Vascular Morphologyare Associated with Fetal Growth and Birthweight: theRotterdam Periconception Cohort, in: 32nd World Congress on Ultrasound in Obstetrics and Gynecology, London, UK & Virtual, 2022, pp. 256–257.
[24] M. Rousian, S. Schoenmakers, A.J. Eggink, D.V. Gootjes, A.H.J. Koning, M.P. H. Koster, A. Mulders, E.B. Baart, I.K.M. Reiss, J.S.E. Laven, E.A.P. Steegers, R.P. M. Steegers-Theunissen, Cohort Profile Update: the Rotterdam Periconceptional Cohort and embryonic and fetal measurements using 3D ultrasound and virtual reality techniques, Int. J. Epidemiol. (2021).
[25] R.P. Steegers-Theunissen, J.J. Verheijden-Paulissen, E.M. van Uitert, M. F. Wildhagen, N. Exalto, A.H. Koning, A.J. Eggink, J.J. Duvekot, J.S. Laven, D. Tibboel, I. Reiss, E.A. Steegers, Cohort profile: the Rotterdam periconceptional cohort (predict study), Int. J. Epidemiol. 45 (2) (2016) 374–381.
[26] L. Drukker, R. Droste, P. Chatelain, J.A. Noble, A.T. Papageorghiou, Safety Indices of Ultrasound: adherence to Recommendations and Awareness During Routine Obstetric Ultrasound Scanning Sicherheitsindizes im Ultraschall: einhaltung der Empfehlungen und Aufmerksamkeit beim Routine-Ultraschall in der Geburtshilfe, Ultraschall Med. 41 (2) (2020) 138–145.
[27] A.D. Reus, J. Klop-van der Aa, M.S. Rifouna, A.H. Koning, N. Exalto, P.J. van der Spek, E.A. Steegers, Early pregnancy placental bed and fetal vascular volume measurements using 3-D virtual reality, Ultrasound Med. Biol. 40 (8) (2014) 1796–1803.
[28] T.Y. Khong, E.E. Mooney, I. Ariel, N.C.M. Balmus, T.K. Boyd, M.A. Brundler, H. Derricott, M.J. Evans, O.M. Faye-Petersen, J.E. Gillan, A.E.P. Heazell, D. S. Heller, S.M. Jacques, S. Keating, P. Kelehan, A. Maes, E.M. McKay, T.K. Morgan, P.G.J. Nikkels, W.T. Parks, R.W. Redline, I. Scheimberg, M.H. Schoots, N.J. Sebire, A. Timmer, G. Turowski, J.P. van der Voorn, I. van Lijnschoten, S.J. Gordijn, Sampling and definitions of placental lesions Amsterdam placental workshop group consensus statement, Arch. Pathol. Lab Med. 140 (7) (2016) 698–713.
[29] Y. Khong, I. Brosens, Defective deep placentation, Best Pract. Res. Cl Ob 25 (3) (2011) 301–311.
[30] G.J. Burton, E. Jauniaux, What is the placenta? Am. J. Obstet. Gynecol. 213 (4 Suppl) (2015) S6–S8. S6 e1.
[31] A.O. Odibo, Y. Zhong, M. Longtine, M. Tuuli, L. Odibo, A.G. Cahill, G.A. Macones, D.M. Nelson, First-trimester serum analytes, biophysical tests and the association with pathological morphometry in the placenta of pregnancies with preeclampsia and fetal growth restriction, Placenta 32 (4) (2011) 333–338.
[32] C.M. Salafia, J. Zhang, R.K. Miller, A.K. Charles, P. Shrout, W. Sun, Placental growth patterns affect birth weight for given placental weight, Birth Defects Res. 79 (4) (2007) 281–288.
[33] C.M. Salafia, M. Yampolsky, D.P. Misra, O. Shlakhter, D. Haas, B. Eucker, J. Thorp, Placental surface shape, function, and effects of maternal and fetal vascular pathology, Placenta 31 (11) (2010) 958–962.
[34] A. Eskild, C. Haavaldsen, L.J. Vatten, Placental weight and placental weight to birthweight ratio in relation to Apgar score at birth: a population study of 522 360 singleton pregnancies, Acta Obstet. Gynecol. Scand. 93 (12) (2014) 1302–1308.
[35] H.G. Herman, H. Miremberg, L. Schreiber, J. Bar, M. Kovo, The association between disproportionate birth weight to placental weight ratio, clinical outcome, and placental histopathological lesions, Fetal Diagn. Ther. 41 (4) (2017) 300–306.
[36] H.J. Liu, P.C. Liu, J. Hua, Y. Zhao, J. Cao, Placental weight and size in relation to fetal growth restriction: a case-control study, J. Matern. Fetal Neonatal Med. 34 (9) (2021) 1356–1360.
[37] D.J.P. Barker, K.L. Thornburg, C. Osmond, E. Kajantie, J.G. Eriksson, The surface area of the placenta and hypertension in the offspring in later life, Int. J. Dev. Biol. 54 (2–3) (2010) 525–530.
[38] N.R. Winder, G.V. Krishnaveni, S.R. Veena, J.C. Hill, C.L.S. Karat, K.L. Thornburg, C.H.D. Fall, D.J.P. Barker, Mother's lifetime nutrition and the size, shape and efficiency of the placenta, Placenta 32 (11) (2011) 806–810.
[39] G.E. Fox, R. Van Wesep, J.H. Resau, C.C. Sun, The effect of immersion formaldehyde fixation on human placental weight, Arch. Pathol. Lab Med. 115 (7) (1991) 726–728.
[40] R. Tambouret, W.R. Jeck, D.J. Roberts, The difference between unfixed and postfixation placental weight, Am. J. Clin. Pathol. 152 (2) (2019) 217–220.
[41] A. Downey, K. Hore, F.M. McAuliffe, E.E. Mooney, Umbilical cord shortening: quantification postdelivery and postfixation, Pediatr. Dev. Pathol. 17 (5) (2014) 327–329.

[42] A.O. Odibo, K.R. Patel, A. Spitalnik, L. Odibo, P. Huettner, Placental pathology, first-trimester biomarkers and adverse pregnancy outcomes, J. Perinatol. 34 (3) (2014) 186–191.
[43] V. Schiffer, C.W.J. Borghans, N. Arts, J.A.P. Bons, C.A.H. Severens-Rijvers, S.M. J. van Kuijk, M.E.A. Spaanderman, S. Al-Nasiry, The association between first trimester placental biomarkers and placental lesions of maternal vascular malperfusion, Placenta 103 (2021) 206–213.
[44] B. Bustamante Helfrich, N. Chilukuri, H. He, S.R. Cerda, X. Hong, G. Wang, C. Pearson, I. Burd, X. Wang, Maternal vascular malperfusion of the placental bed associated with hypertensive disorders in the Boston Birth Cohort, Placenta 52 (2017) 106–113.